Earthquake-induced landslides: complicated mechanisms and outputs

Ikuo Towhata

Visiting Professor, Kanto Gakuin University, Yokohama, Japan

email_towhata.ikuo.ikuo@gmail.com

Abstract

Earthquake-induced landslide is not a new topic and there were many studies in the 20th Century. After those great achievements, a new direction has been shown by experience of gigantic earthquakes toward the end of the 20th Century and at the beginning of the 21st Century. Those big quakes include the 1999 Chi-chi earthquake, the 2008 Wenchuan earthquake, the 2011 Tohoku earthquake and many others. Because those quakes were caused by rupture of very long faults, the former idea of "epicenter" has to be replaced by "rupture zone" now. Compound effects of seismic shaking with rainfall appear to affect the damage extent profoundly. The long-term instability of shaken slopes during the aftermath stage is a new threat to a local community. Landslide dam is also an important threat as well. Because seismic landslide starts near the top of a mountain, the topographic amplification is supposed to trigger land slip via tension/toppling mechanism in place of the conventional idea of shear failure. The importance of tsunamigenic landslide is understood nowadays after several bad experiences. Thus, research and practice of earthquake-induced landslide encounter different problems and are required to pose new viewpoints. In this regard, this paper attempts to introduce what are known to date and exhibit future direction.

1 INTRODUCTION

Earthquake is one of the important types of natural disasters. It may be true that recent decades are experiencing more significant earthquake disasters that the middle 20th Century. In the recent decades, for example, the seismic events in northern Pakistan (2005, moment magnitude, *M*w, = 7.6), Indian Ocean (2004, *M*w=9.1-9.3), Sichuan Province in China (2008, *M*w=7.9) and Tohoku Region in Japan (2011, *M*w=9.0) revealed huge energy to affect human community. Slightly smaller earthquakes hit Taiwan (Chi-chi earthquake, 1999, *M*w=7.6), Turkey (1999, *M*w=7.6), Japan (Niigata-Chuetsu earthquake, 2004, *M*w=6.6), Sumatra (Padang area, 2009, *M*w=7.5), Nepal (Gorkha earthquake, 2015, *M*w=7.8), Japan (2016, Kumamoto, *M*w=6.2 and 7.0 with 28-hour interval), Japan (2018, Iburi-Tobu earthquake, *M*w=6.6), New Zealand (Kaikoura earthquake, 2016, *M*w=7.8) Sulawesi Island of Indonesia (2018, *M*w=7.5) and New Zealand (2010 and 2011, *M*w=7.1 and 6.2, respectively) among many others and affected the resilience of communities as well. It may be reasonable to state that the recent human community is more advanced but less resistant than before due to advanced use of lifelines and expansion into seismically prone regions. Landslide is certainly one of the seismic threats that totally destroy human communities.

The present paper addresses those landslides and slope disasters that were induced by earthquake actions. This topic appears novel and important because of the following reasons.

- The number of victims and negative effects on resilience of affected community are significant as exemplified by the 2008 Wenchuan earthquake in China.
- The substantial damage induced by seismic slope disaster implies that damage mitigation is still underdeveloped.
- Because earthquakes cannot be foreseen, earthquake-induced slope disasters cannot be predicted. This means that early warning and evacuation are not possible in contrast with the gravity-induced landslides and even rainfall-induced slope disasters.

One may even notice that much is not yet known about the mechanical process of slope failures under the seismic action except a brief phrase of "seismic shaking affects the slope stability". This is in clear contrast with the knowledge on gravity-induced landslides where shear deformation and failure play major roles. Moreover, concern is increasing towards the interaction of different natural actions such as earthquake and rainfall that work together to increase the slope instability. This point is called the compound effect in this text.

With these in mind, the present paper reviews recent disasters and summarizes knowledge so far available.

2 EARTHQUAKE-INDUCED LANDSLIDES IN THE RECENT TIMES

2.1 Chi-Chi earthquake in Taiwan, 1999

Caused by rupture of the Chelongpu Fault on September 21, this earthquake registered the moment magnitude of *M*w=7.6. Its damage was characterized by subsoil liquefaction in alluvial planes as well as slope disasters in mountainous regions. A great number of slope failures occurred in Taiwan because

- the geology of the western half of Taiwan Island is young (mostly Cenozoic, being about 23 million years old or younger) and the rocks are not fully solidified yet,
- Taiwan Island is located between the Eurasian and the Philippine Sea tectonic plates, the tectonic stress condition in the island is complicated. Mountains are, therefore, subject to significant distortion that results in joints, cracks and other types of damage.
- the annual precipitation in Taiwan is high (e.g. 2402 mm/year in Sun Moon Lake in mountainous region) and mountain slopes undergo rapid erosion and become very steep,
- the earthquake occurred near the end of the rainy season and the water content in the slopes was most probably very high. Fig. 1 illustrates the mean monthly precipitation in the Sun Moon Lake near the affected region.

Figure 2 shows the slope failure at Tsaoling whose volume was 120 million m^3 (Hung, 2000). Noteworthy is that this slope consists of soft rock layers that are parallel to the slope surface (Hung, 2000). Accordingly, this slope failed several times during past earthquakes in 1862 and then in 1941 (Kawata, 1943) and rainfalls in 1942 and 1979. Because one rock block still remains at the top, one more disaster is likely in near future.

The slope failure in 1941 in Tsaoling with 150 million m^3 of volume produced a natural dam (Kawata, 1943) and the same was repeated in 1999. Because of the possibility of breaching and flooding, natural dam is now attracting serious concern. When the author made his second visit in

2013, the lake had been already filled with sediments and the failed surface was covered by grass. Thus, the recovery of the slope surface was evident in 14 years after the disaster.

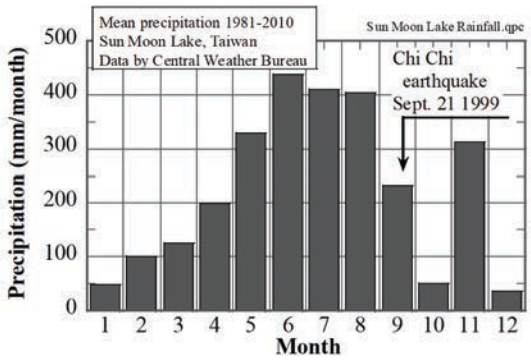

Figure 1. Mean monthly precipitation in Sun Moon Lake that is close to the seismic landslide area (Central Weather Bureau,https://www.cwb.gov.tw/V8/E/C/Statistics/monthlymean.html, retrieved on Feb. 21, 2020)

Figure 2. Failed slope at Tsaoling, Taiwan Island

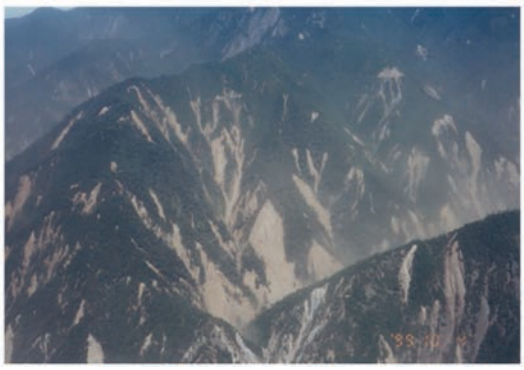

Figure 3. Damage of slope/cliff surface

As stated above, the mountain body is very weak. As a consequence, slope surface slipped down at many places (Fig. 3). It left a huge deposit of sediment at the valley bottom. The repetition of debris flow disasters during the following years due to heavy rain (Lin et al., 2004; Lin et al., 2010) was a natural consequence of this situation.

2.2 Niigata-Chuetsu earthquake, Japan, 2004

The affected area is characterized by young geology together with significant tectonic compression (Kurita, 2010). Accordingly, there had been many ancient landslides before the earthquake and the seismic shaking triggered many land slips. Fig. 4 shows one of them that clearly indicates a circular slip mechanism. Fig. 5 shows that many slopes slipped down due to weak geology. Accordingly, natural dams were formed at many places. In the foreground of Fig. 5, the failed soil mass traveled over some distance in the horizontal direction and blocked the river flow. On the contrary in the back ground, a thinner and smaller soil mass simply dropped down and stopped there, without blocking the river. This finding suggests the effect of soil volume on the horizontal travel distance.

In addition to weak geology in this hilly area, it may be important that the local community had been living on fish farming by which water had probably been supplied into subsoil. Another issue is the effect of antecedent rainfall that occurred due to typhoon 3 days before the earthquake (Tochio and Nagaoka in Fig. 6). Noteworthy is that road embankments in this area were made of locally available crushed mudstone that became soft by absorbing water and slaking, leading to easy failure during the earthquake (Fig. 7). It is supposed that abundant ground water thus provided aggravated the extent of disasters. Because most roads were destroyed, local people could not stay home anymore and had to move out of the hilly area to live in shelters in cities.

Figure 4. Dainichi-yama slope failure during the Niigata-Chuetsu earthquake, 2004

Figure 5. Many slope instabilities in Yamakoshi area caused by the 2004 Niigata-Chuetsu earthquake

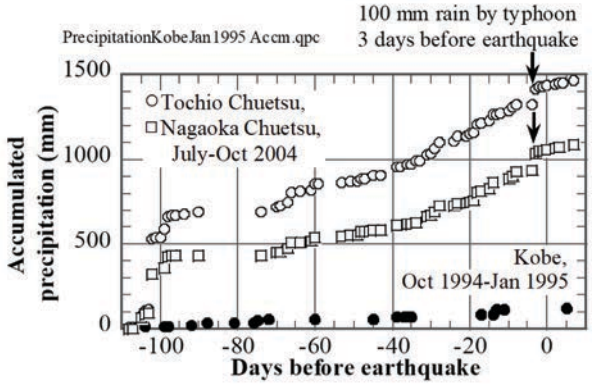

Figure 6. Rainfall record prior to the Niigata-Chuetsu earthquake (recorded in nearby Tochio and Nagaoka Cities in comparison with similar record in Kobe, 1995)

Figure 7. Failed road embankment that was made of crushed mud stone

2.3 Earthquake in Northern Pakistan, 2005

Rupture of the Muzaffarabad Fault caused this earthquake on October 8. Fig. 8 illustrates the dislocation of this fault that is directed towards a slope failure to the north of Muzaffarabad City. Many slopes slipped during this earthquake. Fig. 9 shows the biggest one. The soil mass blocked the river at the bottom and later breached (Konagai and Sattar, 2012). It is important that small but many failures happened along the causative fault (Fig. 10). The author has been particularly interested in the slope instability behind Muzaffarabad (Fig. 11) because this slope was stable immediately after the quake and, afterwards, became unstable gradually with time. Fig. 12 shows the mean monthly rainfall in the area. Because the earthquake occurred at the end of the rainy season, the antecedent rail could have affected the slope instability, while erosion during aftermath is not very likely.

Figure 8. Fault dislocation near Muzaffarabad during the earthquake in Pakistan, 2005

Figure 9. Hattian Landslide that occurred during the Northern Pakistan earthquake in 2005

Figure 10. Many slope failures along the Muzaffarabad Fault in Pakistan, 2005

Figure 11. Slope instability and disappearance of vegetation at Gulshan Nallah near Muzaffarabad that started after the earthquake

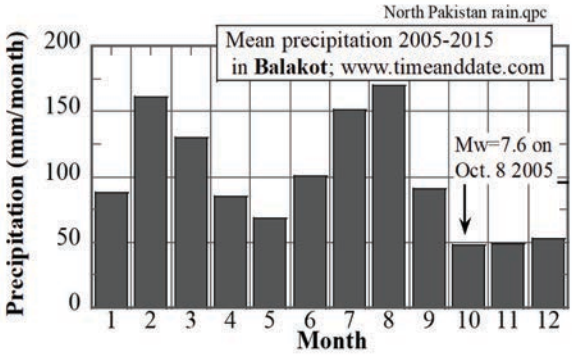

Figure 12. Mean precipitation in Balakot near Muzaffarabad

2.4 WENCHUAN EARTHQUAKE IN CHINA, 2008

The Wenchuan earthquake was induced on May 12th by rupture of the Longmenshan Fault in Sichuan Province. Many buildings collapsed due to their insufficient resistance against seismic loading. Many slopes slipped down and destroyed infrastructures. At the same time, landslide dams were formed at many places.

Figure 13 shows one of the big slope failures where debris flow claimed 60 lives under deposit.

Figure 13. Slope failure at Xiejiadian (謝家店) with grazing angle of 26 deg.

The grazing angle, which is the gradient of a line connecting the head scarp and the bottom end of deposit, was measured to be about 26 degrees while the volume of the debris mass is unknown; being possibly of the order of one million m^3.

Figure 14 shows the event in Donghekou where a huge volume of debris fell down and formed a natural dam. The grazing angle was measured to be 20 degrees.

Beichuan was one of the centers of damage. Fig. 15 indicates a site of slope failure near this town. This slope is made of mud stone and, after the earthquake, it became unstable and many debris flows occurred during rainfall after the earthquake.

Figure 14. Slope failure at Donghekou (東河口) with 10 million m^3 volume and equivalent friction angle of 20 deg.

Figure 15. Slope failure near Beichuan (北川) where debris flows have been repeated after the earthquake

As was mentioned for Taiwan and Muzaffarabad, increase of slope disaster hazard during the aftermath deserves more attention. Fig. 16 demonstrates an example of affected mountain slopes where surface material fell down during heavy rains. Consequently, the valley at the bottom was filled with sediments and the former summer resort there was abandoned.

Figure 17 clearly indicates where the seismic slope failure starts during strong shaking. It started very near the top of a mountain, which is in a clear contrast with the behavior of rainfall-induced slope failures. The latter starts at a nick point at the middle height of a slope where the slope gradient changes from steep slope in the lower part to gentler slope towards the top. The reason

for the finding in Fig. 17 is the concentration of earthquake (shaking) energy towards the mountain top. Figure 18 shows that the earthquake occurred in the early stage of rainy season. Thus, it is possible that antecedent rain exerted only limited effect on slope instability but the post-earthquake rain likely aggravated the disaster.

Figure 16. Mountain slope disturbed by earthquake shaking and valley filled with repeatedly induced debris flows (Yin chang gou 銀場溝)

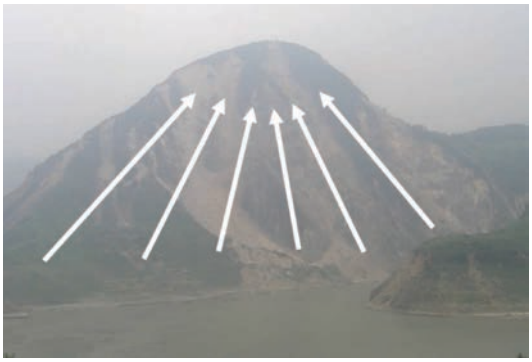

Figure 17. Earthquake-induced slope failure starting from the top of mountain (near Zipingpu Dam reservoir)

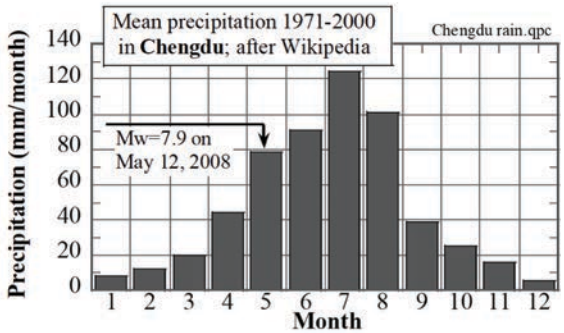

Figure 18. Mean precipitation in Chengdu

2.6 SEISMIC FAILURE OF SLOPES OF VOLCANIC MATERIALS IN COSTA RICA, 2009

Seismic instability of slopes comprised of volcanic materials has not attracted much attention. However, recent experiences suggest that such a slope is highly prone to seismic effect.

The 2009 Cinchona earthquake in Costa Rica on January 8 registered *M*w=6.1 and induced many slope failures in Congo and Poas Volcanos (Barrantes-Castillo, 2013). The surface of the affected slopes is covered by ash and likes.

Figure 19. Failure of slope of Volcán Congo caused by the Cinchona earthquake in Costa Rica

Figure 20. Appearance of Rio Seco in Costa Rica after debris flow

Figure 21. Slope failure starting from the top of ridge (Cinchona)

Figure 19 shows the minor failures in a volcanic slope. Although their size looks small in this photograph, these failures in this mountain blocked a river (Rio Seco) and this natural dam breached by overtopping. The induced debris flow

destroyed a bridge in the downstream area. Fig. 20 looks towards the downstream directiopn of this river whose width increased from 5 m to max. 20 m due to erosion. Similar to Fig. 17, the slope failure in Fig. 21 started from the ridge, not from the nick point. This was a substantial problem to local communitoies that were situated at the ridge.

The mean precipitation in the mountain region of Costa Rica is illustrated in Fig. 22. It is found herein that the earthquake occurred during the dry season. This seems fortunate and, if the earthquake had occurred near the end of the rainy season, the slope disasters would have been substantially more serious. The problem of rainfall on slopes of volcanic materials will be repeated in what follows.

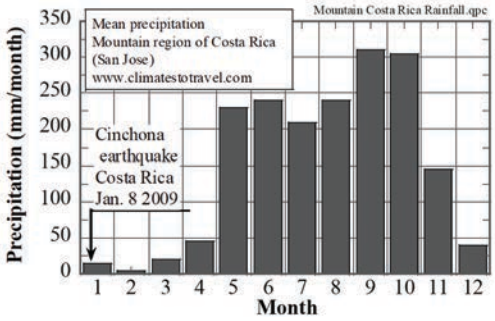

Figure 22. Mean precipitation in mountain region of Costa Rica (San José)

2.7 SEISMIC FAILURE OF SLOPES MADE OF VOLCANIC MATERIALS IN SUMATRA, INDONESIA, IN 2009

Padang is located on the western coast of Sumatra Island, Indonesia, where a sequence of huge earthquakes occurred after the tsunami-genic event in 2004. The event in 2009 induced building collapse and subsoil liquefaction in Padang City together with many slope failures in its suburbs.

Near Padang, there are several volcanos such as Tandikat and slope surface in the affected area is covered by scoria that originated from those volcanos. Fig. 23 illustrates one of the slope failures in Palakoto locality where 41 residents were killed under the flow failure. This disaster is characterized by a long-distance run-out along nearly level ground surface. Fig. 24 shows the deposit of the failed soil mass that is composed of coarse brownish grains and was judged to be scoria. The volume of flow failure was assessed on the soil mass in Malakak community (Fig. 25) to be about 0.4 million m^3.

Evidently, the induced slope failures were affected by the ample amount of ground water as a consequence of rainfall. Figure 26 shows that the Padang area has high precipitation all the year around (4372 mm per year on average). When the author visited the site in November, 2009, a heavy shower started and the steep slope in front of the author flowed down (Fig. 27). Its appearance was similar to flow of viscous liquid, which was very impressive to the author.

Figure 23. Destroyed community of Palakoto, Indonesia

Figure 24. Deposit of flow material in Palakoto

Figure 25. Flow failure at Malakak, Sumatra Barat, Indonesia

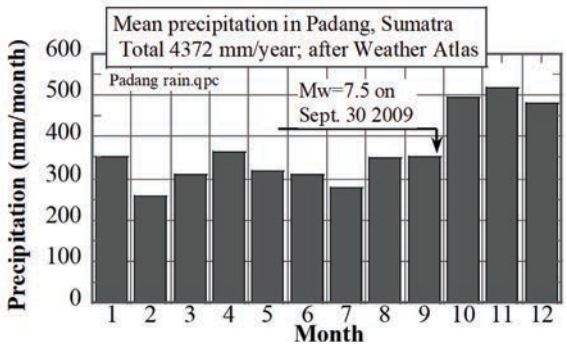

Figure 26. Mean precipitation in Padang, Sumatra Barat, Indonesia

Figure 27. Small mountain near Cumanak where "viscous" flow occurred during heavy shower

2.8 SEISMIC FAILURE OF SLOPE MADE OF VOLCANIC MATERIALS IN TSUKIDATE, JAPAN, IN 2003

The previous sections addressed slope instability of volcanic materials. Kazama et al. (2006) studied the cyclic behavior of volcanic ash to show that water is held in ash grains and is released during cyclic shear deformation, thus making the slope unstable. This behavior becomes serious if ample ground water is available in slopes. Most probably this was the case in events in Padang.

The 2003 Miyagiken-oki earthquake of *M*w=7.0 in Japan triggered a slope failure in Tsukidate Town near Sendai City. Fig. 28 illustrates the view of the sliding mass seen from the bottom. This site used to be a small valley and was filled with locally available volcanic ash deposit. In spite of gentle sloping, the soil mass traveled over a long distance. One reason for this is the weakness of the soil as Kazama stated, while the other reason is that the soil mass was able to travel along rice paddy (Fig. 29) whose surface is covered by very soft mud and allows nearly free sliding in the horizontal direction. In countries of rice agriculture, the softness of rice paddy deserves attention.

Figure 28. Site of volcanic fill flow in Tsukidate, Japan, in 2003 (seen from the foot of slope)

Figure 29. Soil mass with bamboo on that traveled onto soft rice paddy (Tsukidate, 2003)

2.9 SEISMIC FAILURE OF SLOPES MADE OF VOLCANIC MATERIALS IN KUMAMOTO, JAPAN, IN 2016

The 2016 Kumamoto earthquake triggered many landslides in the caldera of Aso Volcano. The caldera measures 25 km in North-South diameter and its population is 70,000 approximately. Fig. 30 indicates a big slope failure in the inner slope of the outer rim of the crater. This slope failure destroyed a big bridge at the bottom. Fig. 31 shows a failure of a gentle slope consisting of volcanic materials (Mukunoki et al., 2016). The author measured here the grazing angle to be 16 to 18 degrees.

This earthquake posed several engineering problems. One was the effect of fault displacement under human community. The

second was the long duration of aftershocks (Fig. 32). This situation caused fear among people that a bigger earthquake was coming soon.

Figure 30. Slope failure and destroyed bridge in outer rim of Aso Volcano

Figure 31. Failure of gentle slope made of volcanic materials in Aso

The third problem concerned the latest principle of earthquake-resistant design of many structures. On April 14th and 16th, two very strong shaking affected the epicentral area. The first shakings (foreshock) caused some plastic deformation in structures but did not cause fatal collapse as intended by the design. However, plastic deformation meant partial loss of seismic resistance and, therefore, many structures collapsed fatally upon the second shaking (main shock) 28 hours later. This was against the latest design principle that plastic deformation is allowed under rare strong shaking but fatal collapse is not. To date, no good idea on seismic resistance against two consecutive strong shaking has been proposed. Most probably, many slopes were partially damaged by the first shaking and collapsed upon the second shaking.

Figure 33 illustrates the rainfall record before the earthquake. There was a strong rain one week before the main shock and it possibly affected the stability of volcanic deposits undergoing shaking.

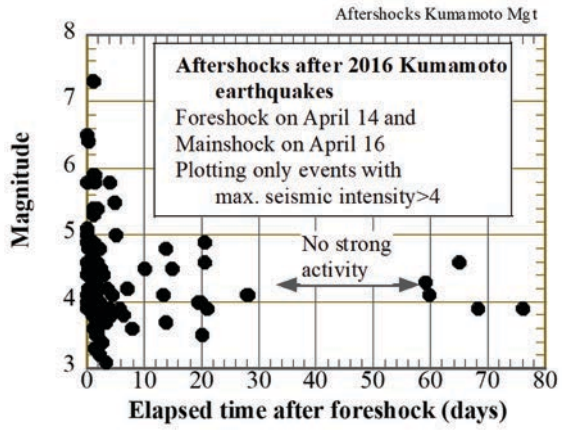

Figure 32. Aftershocks of Kumamoto earthquake

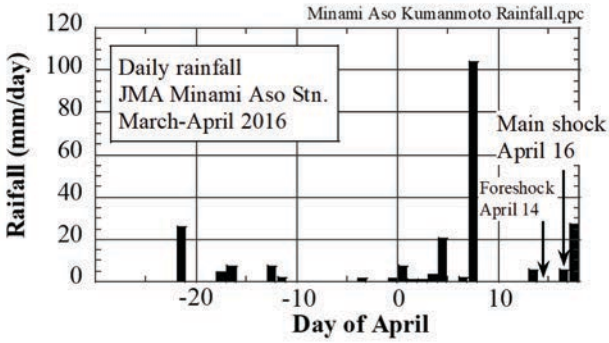

Figure 33. Rainfall record at Minami Aso Station of JMA

2.10 SEISMIC FAILURE OF SLOPES MADE OF VOLCANIC MATERIALS IN ATSUMA of HOKKAIDO, IN 2018

The 2018 Iburi-Tobu earthquake occurred in Hokkaido, Japan, and registered *M*w=6.6. While this earthquake caused collapse of residential fill in Sapporo and the blackout of electric power supply in the Hokkaido Island, the present text addresses the enormous slip failure of volcanic ash slopes in Atsuma Town near the epicenter. Note that Fig. 34 shows only one part of the affected area. Fig. 35 demonstrates the situation in which several houses were buried under the landslide mass. The soil volume is of the order of 10,000 m^3. Note that long-distance flow was made possible by the rice paddy.

The side face of the failed slope in Fig. 36 shows that the slope consists of many layers of volcanic ash that came from eruption of different volcanos. Chuo Kaihatsu Corporation for which the author is a technical advisor made a brief measurement of the strength of ash layers during their reconnaissance and determined the location of slip plane. Fig. 37 indicates the rainfall record for 5 years. Although the rainfall in 2018 was not

particularly high, the event about two weeks before the earthquake (▼) possibly affected the slope instability to a certain extent.

Figure 34. Satellite photo of many failures in volcanic slopes in Atsuma Town (photo by the Cabinet Secretariat)

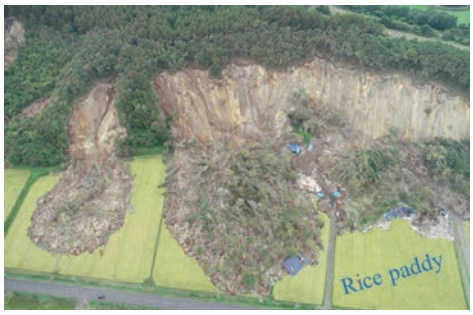

Figure 35. Aerial photo of slope failure in Yoshino District in Atsuma (by Chuo Kaihatsu Corporation)

Figure 36. Cross section of failed slope in Yoshino District

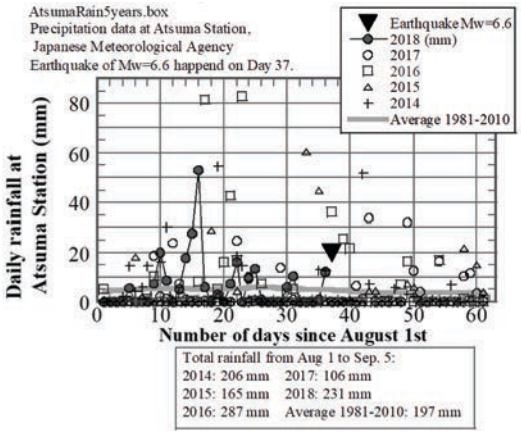

Figure 37. Rainfall data in Atsuma for 5 years

2.11 SEISMIC FAILURE OF SLOPES MADE OF AEOLIAN SOIL

Slopes made of aeolian deposit is known to be unstable during earthquakes. In northwestern part of China, such a material called loess is prevalent. When the 1920 Haiyuan (海原) earthquake of magnitude = 8 hit the Gansu (甘肃) Province, China, slopes of gentle gradient slipped down profoundly (Zhang and Wang, 2007; Wang et al., 2010).

Figure 38 shows one of the places where a gentle loess slope flowed down during the Haiyuan earthquake and blocked river flow. Note that the topography after the disaster has been repaired afterwards. Zhang and Wang (2007) carried out ring shear tests on loess specimens to demonstrate that excess pore water pressure develops profoundly during undrained shear and reduces dramatically the shear strength of the material. Because of the dry climate, loess slope is subject to instability when wetted by, e.g., overirrigation (Zhang et al., 2009).

Figure 38. Site of loess landslide caused by Haiyuan earthquake (西吉 Xiji, Ningxia, China)

2.12 SEISMIC FLOW FAILURE OF ALLUVIAL FAN SLOPES IN PALU, SULAWESI ISLAND, INDONESIA, IN 2018

On September 28th, 2018, the central part of Sulawesi Island, Indonesia, was hit by an earthquake of *M*w=7.5. This earthquake is characterized by two damage mechanisms. The one is submarine landslide that triggered tsunami in the coastal area. The other is the gigantic flow failures in which surface soil traveled more than 500 meters in spite of the gentle slope angle of 1 degree or so (Irsyam et al., 2018). The author has been fully involved in the international research activities addressing the causative mechanism of this long-distance flow and hazard mapping methodology. However, it is difficult to publish the output at this moment due to the governmental agreement on publication. A limited amount of information was discussed by Kiyota during the 7th Int. Conf. Earthquake Geotechnical Engineering in Rome (June, 2019). In this paper, the author pesents only what he thought personally on this disaster.

The important point is that sandy slopes of very small gradient displaced 500 meters. This is completely different from what has been known on liquefaction; lateral displacement was at maximum 10 meters or so even in significant extent of liquefaction. It was a big surprise that a tremendous lateral displacement happened at 4 sites around Palu; Balaroa, Petobo, Jono Oge and Sibalaya, while Lolu site developed displacement less than 100 m. The question is why such a rare phenomenon of huge lateral dispalcement happened at 4 (or 5) places at the same time. The major points in the author's mind are as what follows;

- The subsoil had plenty of ground water that was supplied from the alluvial fan topography as well as irrigation (no irrigation in Balaroa site).
- In addition to liquefaction in the surface soil, artesian water pressure from the upper part of alluvial fan may have promoted lateral flow.
- Water film caused by redistribution of excess pore water pressure after liquefaction (Kokusho, 2000) may have promoted lateral flow.
- Konin earthquake in Japan (AD 818, Magnitude = 7.9) triggered substantial cracks and flow failures in a vast scale in alluvial fans (Hayakawa et al., 2002). Its possible similarity with the disaster in Indonesia deserves attention.
- Palu-Koro Fault may have played some role in the flow failure.
- Whatever idea may be proposed on the damage mechanims, it should not be a commonly observed situation because what happened is very rare.
- Is it possible to quantitatively understand the long-distance flow in such a gentle sloping ground?

2.13 SEISMIC FAILURE OF MOUNTAIN SLOPES IN NEW ZEALAND DURING THE KAIKOURA EARTHQUAKE IN 2016

This earthquake triggered many slope failures along the causative fault. Because the number of slope failure was as many as 10,000, studies on details of slope disasters are still underway (Dellow et al., 2017; Jibson et al., 2017; Massey et al., 2018). The induced damage consists of slope slip, blocking of rivers and breaching that destroyed transportation infrastructures.

Figure 39 shows one of the major landslides at Leaders. This slope failure occurred in greywacke that is of many joints and cracks. Note that the soil mass stopped the river flow (bottom left of photo). This natural dam was still stable when the author visited the site in January, 2020, which was more than 3 years after the earthquake.

Figure 39. Leaders landslide in greywacke caused by the Kaikoura earthquake

Figure 40. Linton landslide and breached natural dam

Figure 41. Seafront slides in limestone

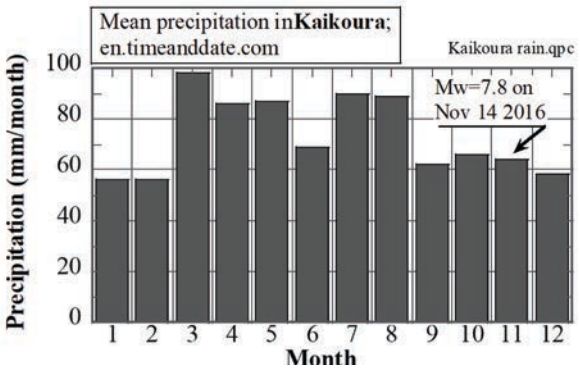

Figure 42. Mean rainfall record in Kaikoura

Figure 40 indicates the Linton landslide that is of 2 million m^3 in volume and blocked river. This natural dam breached later. Fig. 41 depicts slope failure in limestone area near the sea shore. In the Kaikoura area, the monthly rainfall is similar around the year (Fig. 42).

2.14 SEISMIC FAILURE OF MOUNTAIN SLOPES DURING THE 2011 TOHOKU EARTHQUAKE IN JAPAN

It was remarkable that the number of landslides caused by the gigantic 2011 Tohoku earthquake in Japan was small in spite of its big magnitude (*M*w=9.0) and the strong acceleration with long duration time. Fig. 43 illustrates the seismogram recorded at the K-Net Ishinomaki station that is close to the epicenter (beginning of rupture) of this earthquake. Because the maximum acceleration was powerful, the duration of shaking exceeded 150 seconds including more than 80 cycles of loading.

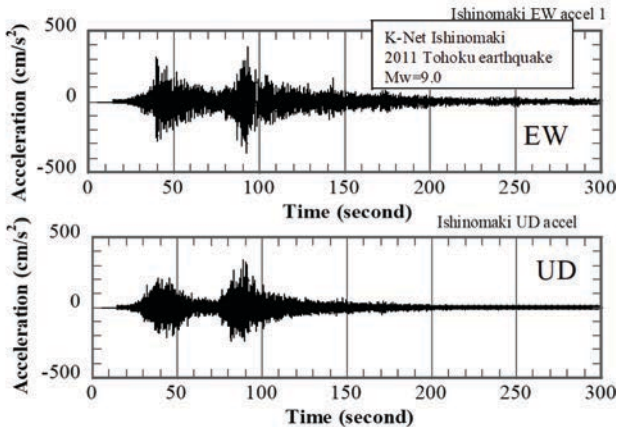

Figure 43. Acceleration records at K-Net Ishinomaki near the epicenter

This paper introduces two sites of slope instability during this earthquake. Fig. 44 shows one of the biggest landslides that occurred at Hanoki-Daira in Shirakawa City south of Sendai. The grazing angle at this site was 5 degrees. Chigira et al. (2012) stated that this slope comprised of such volcanic materials as pumice, scoria and ash while the volume of this sliding mass was 30 thousand m^3.

Figures 45 and 46 compare two slopes in Kotobuki-Yama area in Shiroishi, near Shirakawa. The 1978 Miyagiken-oki earthquake of *M*w=7.5 triggered substantial slope failure here. This site was composed of volcanic fill materials and the size of the failure in 1978 was 70000 m^3 with the grazing angle of 11 degrees (Kobayashi, 1980). After the disaster, the failed slope was restored by installing substantial drainage facilities. Accordingly, no failure happened in 2011 here; see vertical wells for drainage in Fig. 45. In contrast, another slope in its vicinity developed many cracks and displacement in 2011 (Fig. 46). The experiences in 2011 implies the risk involved in earth filling by volcanic materials.

In spite of some slope disasters mentioned above, it has been felt that the number of slope disaster during the 2011 Tohoku gigantic earthquake was less than anticipated from the intensity of shaking. One reason for this is the shortage of rainfall in the Pacific Coast region prior to the earthquake. Fig. 47 illustrates the record of precipitation in Sendai City in every 1/3 of month. The small number of landslide disaster is in clear contrast with the abundant damage caused by subsoil liquefaction under the surface where plenty of ground water was available (Towhata, 2019).

Figure 44. Slope failure at Hanoki-Daira during the 2011 Tohoku earthquake

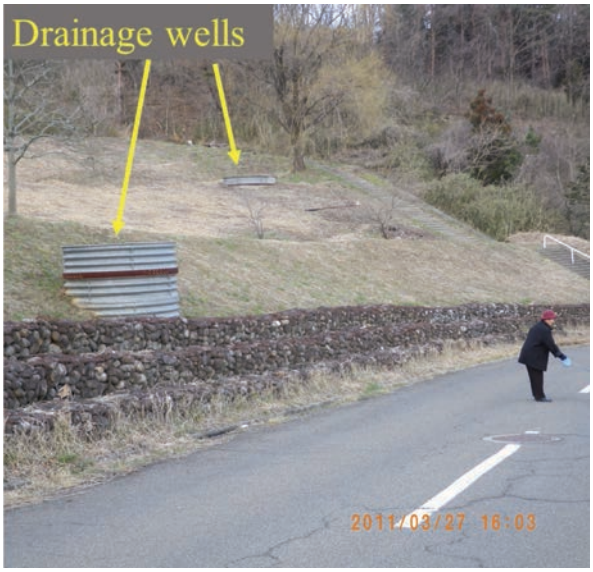

Figure 45. Intact slope in Kotobuki-Yama site in Shiroishi City where drainage facilities had been installed

Figure 46. Slope failure in Kotobuki-Yama during the 2011 Tohoku earthquake

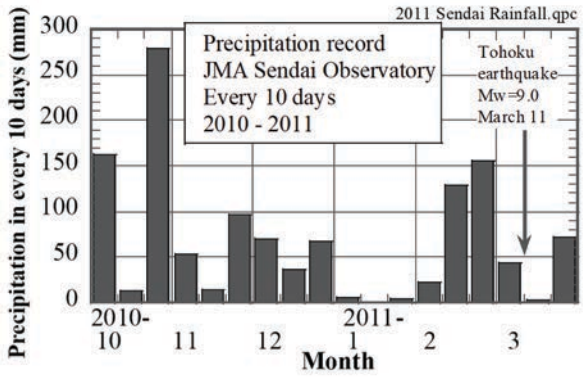

Figure 47. Rainfall record in 2010-2011 in every 10 days at JMA Sendai Observatory

3 DISCUSSION ON FAILURE MECHANISM OF SLOPES UNDER SEISMIC LOADING

As a custom of seismic response analysis, structures subject to seismic loading are analyzed by applying seismic force, whether dynamic or pseudostatic, in the horizontal direction. The additional seismic vertical load may or may not be employed. In case of slopes, seismic safety is then judged by examining the shear stress and strength in a potential slip plane. Thus, the basic hypothesis is that earthquake-induced landslide is a consequence of shear failure of soils and rocks. There are, however, several studies that are not consistent with this traditional hypothesis.

The local governemnt of Kanagawa Prefecture (1986) that is situated to the southwest of Tokyo, Japan, proposed a methodology for seismic fragility analysis on natural slopes by interpreting the cases during the 1923 Kanto earthquake of *M*w=7.9-8.2. After statistic interpretation of many cases, it was proposed to assess the fragility (number of possible slope failures within a 500-meter square grid) by using the maximum surface acceleration during future (design) earthquakes, length of a contour line at mean elevation in a grid, difference between the highest and lowest points in a grid, “hardness of local rock/soil”, length of faults, length of artificial slopes and shape of slope (convex or concave).

What is interesting therein was that the hardness index suggested higher vulenrability for hard rock, while less proneness to soil. This is contradictory to the order of shear strength of rock and soil. It seems that rock slope is more resistant against seismic loading than soil slope. The author used to say that this contradiction is because of statistics in which more rock slopes data was emplyed than soil slopes. Mathematics found

more failures in rock slopes than soil slopes. Unstable soil slopes had failed during heavy rain and only very stable soil slopes remained at the time of the earthquake in 1923. This idea may have to be changed now because slope failure may be induced not only by shear but also by toppling and/or tension mechanisms in jointed rock mass.

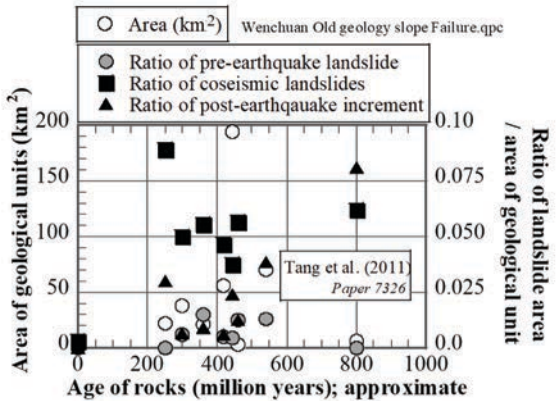

Figure 48. Effects of age of rock on susceptibility to seismic landslide during the Wenchuan earthquake (Tang et al., 2011).

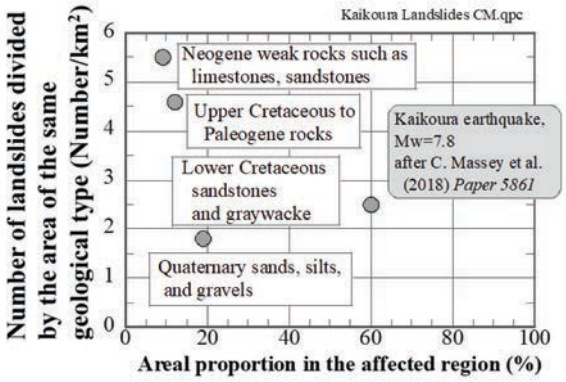

Figure 49. Effects of age of rock on susceptibility to seismic landslide during the 2016 Kaikoura earthquake (Massey et al., 2018)

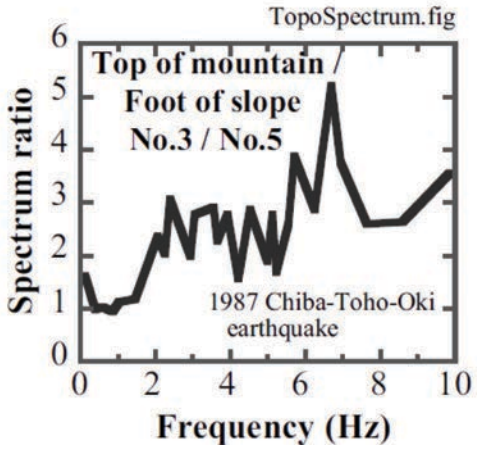

Figure 50. Observed topographic effects on seismic amplification (drawn after Kurita et al., 2005)

Tang et al. (2011) interpreted the feature of slope failures during the 2008 Wenchuan earthquake. In Fig. 48, the areal ratio of seismic landslide slope over the entire area of the same geologic age increases with age; the older, the more landslides. This is particularly evident for slope failures in the post-earthquaek phase. Similar points were made by Massey et al. (2018) on slope failures during the Kaikoura earthquake (Fig. 49). Thus, slopes of geologically older rocks are more susceptible to failure than those of younger soils and rocks.

Figure 17 demonstrated that earthquake-induced slope failure often starts from the top part of mountains. Many other photographs in this paper suggest the same idea. Kurita and Annaka (2005) recorded seismic motion at the top and foot of a mountain and calculated the spectral ratio (amplification) as illustrated in Fig. 50. This figure shows that the motion at mountain top becomes greater with the increase in shaking frequency. This supports the observation in the above-mentioned photographs.

Tang et al (2011) also examined the slope angle at landslide sites. It was found that the pre-earthquake landslides are distributed in the range of 20 to 40 degrees, whilst the coseismic and post-earthquake landslides are in the range of 30 to 50 degrees. This implies either that the static stability (prone to shear failure) at higher slope gradient is marginal, allowing easy seismic failure, or possibly that a different mechanism of seismic shear failure occurs.

Combining the above-mentioned information, the author proposes the importance of tensile or toppling failure mechanism in addition to conventional shear failure mechanism. Toppling is important, for example, in cliff failure (Massey et al., 2017) where the slope angle is high and the

rock mass is prone to tensile failure or separation due to toppling. Fig. 51 schematically illustrates the toppling deformation of a mountain body. This deformation may be associated with subsidence at the top, forming a double ridge. Fig. 52 shows such a deformation at the top of Ohya Mountain, Shizuoka, Japan, where mountain has been creeping and is frequently prone to slope disaster during heavy rains.

In summary, rigid rock mass is prone to earthquake-induced slope failure if the rock mass has many joints/cracks in vertical direction (Fig. 53) and the horizontal seismic acceleration is strong. Separation of rock block reduces the contact and shear strength along the slip plane as well (Fig. 54). Such a situation is not rare near the mountain top where the slope gradient is high.

Another perspective on mechanism of slope failure addresses the *H/L* ratio that is plotted against the volume of landslide mass, *V*. Herein, *H* stands for the vertical fall of landslide mass, while *L* is the horizontal travel distance. Theoretically, *H/L* is equal to tanφ in a slip plane (Hsü, 1975), while φ is the friction angle in terms of total stress; derivation available in Towhata (2008).

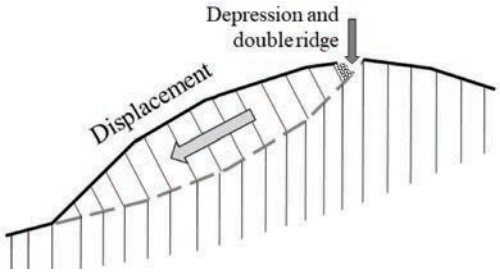

Figure 51. Schematic diagram of toppling deformation

Figure 52. Double ridge and depression at the top of Ohya Mountain, Japan

Figure 53. Slope with vertical separation being prone to toppling failure (Rarangi, New Zealand)

Data from many onshore landslides are plotted in Fig. 55 in order to compare the behavior of non-seismic (Sect. 15.8 in Towhata, 2008) and seismic landslides. Herein, the data on earthquake-induced landslides were collected from Daguangpo during the 2008 Wenchuan earthquake (after p. 64, "*Earthquake-Induced Landslides*" published by the Japan Landslide Society, 2011), Miyagiken-oki earthquake (1978; Kobayashi, 1980), Chi-chi earthquake (Hung, 2000; Chang et al., 2005), Niigata-Chuetsu earthquake (Yagi et al., 2007), Tohoku earthquake (Chigira et al., 2012), and Mitaka-Iriya landslide during the 1978 Izu Oshima Kinkai earthquake of *M*w=6.6 (Kobayashi, 1980) together with the author's own study on Niigata-Chuetsu earthquake and Iburi Tobu earthquake (Fig. 35). It may be seen in Fig. 55 that there is no significant effect of seismic loading on the friction angle except a limited extent of reduced reduction in *H/L* for the volume range of 10^6 – 10^8 m^3. The minor effect is probably because earthquake loading affects the onset of slope failure but does not affect the movement of the earth mass. Certainly, more study is needed on this issue.

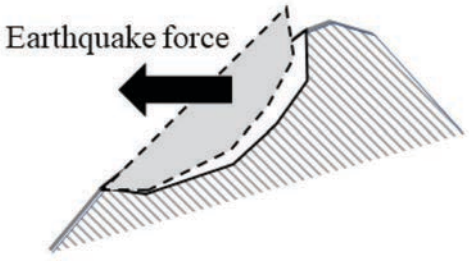

Figure 54. Schematic illustration of separation of rock mass near mountain top due to very strong horizontal seismic force

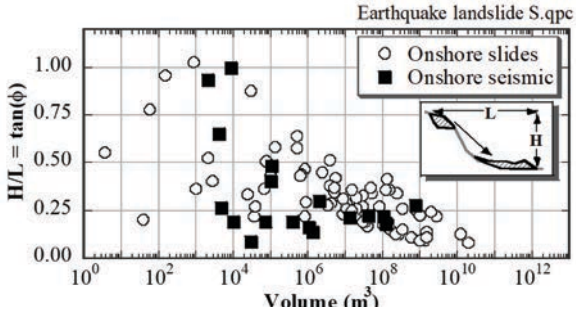

Figure 55. Diagram of *H/L* versus landslide volume

4 EFFECTS OF ANTECEDENT RAINFALL ON SEISMIC SLOPE INSTABILITY AS A COMPOUND EFEFCT

Chapter 2 repeatedly presented the precipitation records in the area of earthquake-induced landslides because high water content in the subsoil increases the weight and reduces the effective stress, leading to smaller factor of safety. In reality, many earthquake-induced landslides are the consequences of combined effects of static failure mechanism and the seismic effect. In other words, the combination of static and seismic stresses exceeds the material strength upon slope failure.

The 2004 Niigata-Chuetsu earthquake of *M*w=6.6 was preceded by ample precipitation (Fig. 6) and induced many landslides in slopes made of soft mud stone etc. In contrast, the 1995 Kobe earthquake of *M*w=6.9 did not cause many slope failures although the local mountains (Mt. Rokko etc,) are made of weathered unstable granite that has been causing many slope disasters during heavy rain (in 1938 and 1967, for example). Fig. 6 was drawn to understand this difference; much less rainfall had occurred in Kobe before the earthquake.

Ground water is provided not only by precipitation. Another significant water source is leakage from nearby reservoir and irrigation channels as well as from broken water pipes and sewage lifelines. Poor treatment of waste water is certainly a problem.

5 NATURAL DAM

Natural dam produced by a landslide mass is a threat to downstream community because its possible breaching causes very powerful debris flow and flood. It is therefore important to search possible dam formation after earthquakes or heavy rain and, if it is found, appropriate safety measure has to be resumed.

It is empirically known that some of natural dams breach while others get stabilized. The Tsaoling Lake was stable after the disaster in Fig. 2. The Diexi Lake in Sichuan Province of China was created at the time of the 1933 earthquake of surface magnitude = 7.5 (Fig. 56) and has been stable until today. Fig. 57 illustrates another seismic lake in Kanagawa Prefecture, Japan, that was formed by a small landslide during the 1923 Kanto earthquake of *M*w=7.9-8.2.

Costa and Schuster (1985) classified causes of natural dam breaching and demonstrated that most dams are destroyed by overtopping (Fig. 58). They also showed that 50% of studied natural dams fail within one week and 85% of dams last for less than one year. So, 15% of dams survive for more than one year. According to a more recent study, most breaching of natural dams is caused by overtopping, while failure by seepage or piping under the dam body is not often the case (Fig. 59). Possibly, natural dam is long in the direction of river (Fig. 60) as compared with the depth of impounded water (Fig. 61), thus blocking small streams and preventing its breaching.

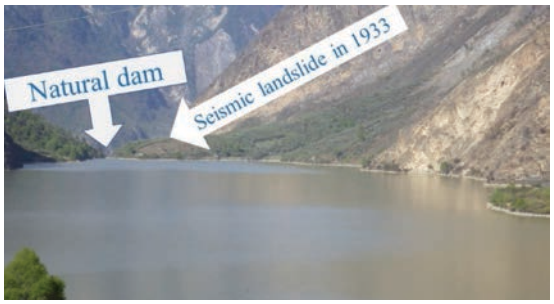

Figure 56. Seismic natural dam and Diexi Lake (叠溪海子) in Sichuan Province

Figure 57. Seismically created Shinsei Lake in Kanagawa, Japan

The possibility of breaching can be assessed by using geometric data on natural dam and

impoundment. Ermini and Casagli (2002) proposed to assess the dam stability by using $\log_{10}[Vd/(A\times Hd)]$ where Vd stands for the dam volume, A the area of catchment and Hd the dam height. The greater this index is, the more stable is the natural dam; stable if > -2.75 and unstable if <-3.08. This empirical method was obtained from worldwide data collection. The author feels, however, that the area of catchment, A, may have to be adjusted to consider the local intensity of precipitation.

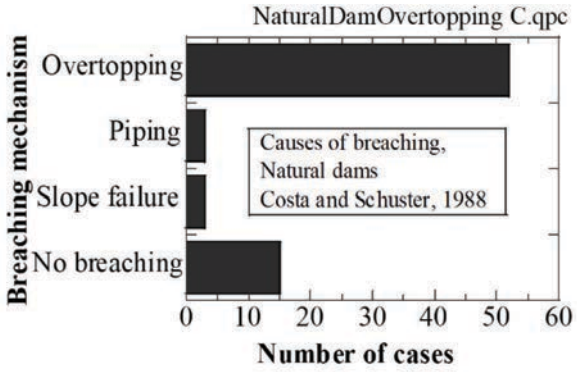

Figure 58. Causes of natural dam breaching (Costa and Schuster, 1988) (inclusive of both seismic and non-seismic cases)

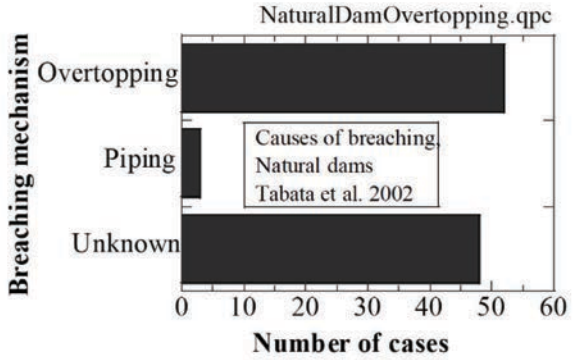

Figure 59. Causes of natural dam breaching (Tabata et al., 2002) (inclusive of both seismic and no

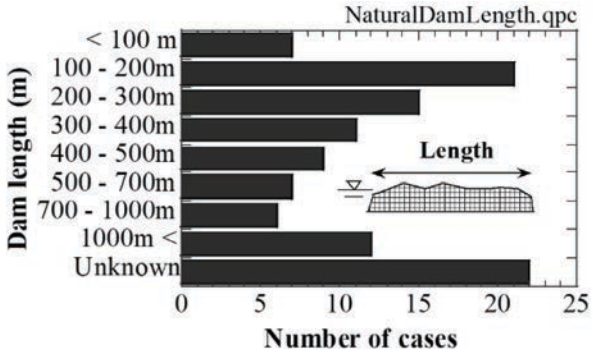

Figure 60. Length of natural dams (Tabata et al., 2002) (inclusive of both seismic and non-seismic cases)

If a natural dam is judged to be unstable, the impounded water has to be removed. Fig. 62 shows ongoing drainage. To avoid erosion of dam body, the drainage channel was protected by steel plates. After the Wenchuan earthquake in China, dams were destroyed by blasting and the cities in the downstream area were evacuated in order to protect human lives from debris flow and flood. Because the mountain slope appeared still unstable and the risk of repeated natural dam formation was high, a drainage tunnel was constructed under the mountain slope (Fig. 63).

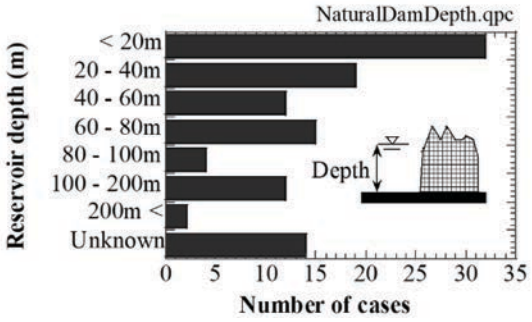

Figure 61. Depth of impoundment in natural dams (Tabata et al., 2002) (inclusive of both seismic and non-seismic cases)

Figure 62. Drainage channel in Terano natural dam after the 2004 Niigata-Chuetsu earthquake

Figure 63. Exit of emergency drainage tunnel next to possible site of future natural dam (唐家山 Tangjiashan natural dam site, Sichuan Province, China)

6 LONG-TERM INSTABILITY OF SLOPES AFTER STRONG SEISMIC EVENTS

Chapter 2 introduced post-earthquake slope disasters. In Taiwan and Pakistan, slope instability and disasters such as debris flow continued for many years (Wang et al., 2003). Lin and Chiang (2019) stated that slope stability looks recovered to some extent 10 years after the earthquake. During the ten years, many typhoons brought heavy rain to Taiwan Island, including the Morakot Typhoon in 2009 with maximum 3000 mm precipitation in 4 days. Fig. 64 shows the amount of siltation (sediment transport) into Tsengwen Dam Reservoir in Taiwan that changed with time in the past decades. Although not clear, it may be possible that the frequency of big siltation event increased after the 1999 Chi-chi earthquake, suggesting the unstable situation in the upstream mountain slopes.

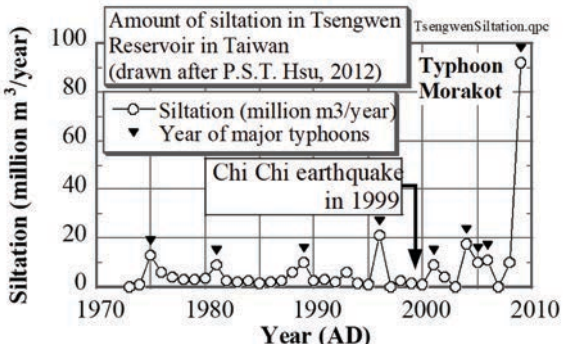

Figure 64. Siltation data in Tsengwen Dam in Taiwan

After the 2008 Wenchuan earthquake in China, many landslides happened in the affected area in 2008-2010 (Li et al., 2012). Afterwards, the slopes in the affected area look recovering seven-ten years after the disaster (compare Figs. 65 and 66). It appears that slopes in Sichuan Province is recovering faster than Taiwan slopesin site of similar seismic damage ane weak geology probably because Taiwan has more rainfall.

The experiences after big earthquakes in the past suggest the following mechanisms of long-term slope instability. First, strong shaking produces many cracks in the mountain slope from which surface water seeps into subsoil and reduces the shear strength of soil and, at the same time, increases the soil weight. Fig. 67 shows such a situation in Pakistan. Second, a huge amount of debris that came down from mountains to the bottom of valleys is washed out during rains. This point was made in relation with the case in Taiwan (Fig. 3). Fig. 68 illustrates the valley of Qingping (清平) which is located in the downstream area of the gigantic Daguangpo (大光包) landslide (Fig. 69; 750 million m^3) that was triggered by the Wenchuan earthquake. It is noteworthy that the Qingping flood did not cause much damage to human community because the local police was on alert and ready for evacuation after a similar rain-induced disaster one week before in Zhouqu (舟曲) of Gansu Province that claimed 1500 victims or more.

Figure 65. Total collapse of mountain slopes along the causative fault valley, Yingxiu 映秀, after the Wenchuan earthquake (photograph taken in June 2008)

Figure 66. Recovery of vegetation on the slope surface near Yingxiu (photograph taken in May 2018)

Figure 67. Surface crack in Northern Pakistan near the site of Hatian Landslide

Figure 68. Qingping valley deposit that was washed out by rain in 2010

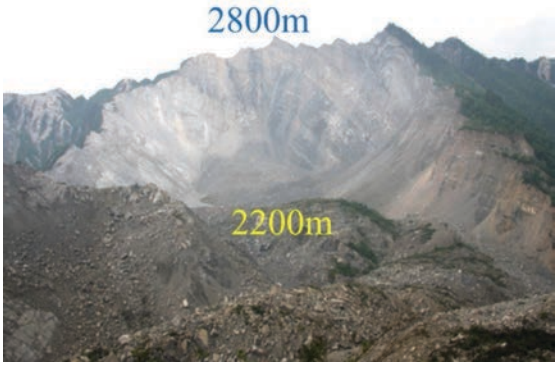

Figure 69. Daguangpo seismic landslide that measured 750 million m^3 in volume (courtesy of the Institute of Mountain Hazards and Environment, Chengdu, China)

Figure 70. Ohya landslide viewed from its top

The discussion is now focused on Ohya landslide in Shizuoka, Japan, that is located at about 100 km west of Tokyo. This site is situated close to the Itoigawa-Shizuoka tectonic line that crosses the Honshu Island of Japan and has been the site of significant geological activities (Naumann, 1885). Fig. 70 shows the appearance of the Ohya landslide that was most probably triggered during the 1707 Hoei earthquake of *M*w = 8.7-9.3 and the volume of the failed mass was about 94 million m^3 (Tsuchiya and Imaizumi, 2010). Since then, this slope has been failing many times during heavy rains. Thus, this site is an example of long-term slope instability that has lasted for 300 years.

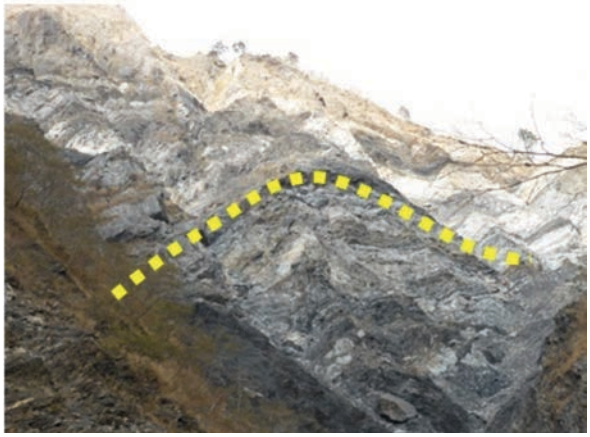

Figure 71. Folding in Ohya Mountain surface

Mokudai and Chigira (2004) studied the creep deformation of the unstable slope in Ohya, Japan. Fig. 71 indicates folding deformation of the Ohya Mountain. Because there are many faults near the Ohya site, this mountain has been subject to continuous action of tectonic stress. Deformation thus produced in the mountain together with the substantial impact during the Hoei earthquake probably developed many cracks and weakness in mountain body and they have been causing long-term slope disaster.

7 FAULT AND LONG-TERM SLOPE DISASTER

Keefer (1994) pointed out the importance of long-term slope disasters that last for years after big earthquakes. While his research interest at that time was in the total vlume of slope failure both during and after earthquakes, Towhata and Gunji (2018) is more interested in the mechanism of the long-term disaster as stated in the previous chapter. To shed light on this, they conducted unconfined compression tests on specimens of artificial rock-like samples in order to study the

effects of creep and major/minor seismic actions on mechanical strength. Unconfined compression tests were considered relevant because the in-situ slope surface undergoes very low overburden pressure. Artifical and uniform specimens were employed to attain similar material properties among all samples that could not be achieved in natural rock specimens.

Figure 72 illustrates the obtained stress-strain behaviors of specimens that underwent cyclic compression prior to the monotonic loading up to failure. It is found herein that preliminary cyclic loading reduces the peak strength, depending on the magnitude and the number of cycles during the preliminary phase. This mechanical damage becomes significant when the deformation caused by the cyclic loading exceeds the strain at peak strength as induced by simple monotonic loading (without cyclic loading). This issue is more evidently demonstraetd in Fig. 73 where the stress-strain states at the end of foregoing cyclic loading (○) and at the peak strength in the monotonic phase (●) are plotted. Most probably, similar phenomena happens during strong earthquakes to trigger long-term instability.

Study was continued by running creep loading under static shear (deviator) stress. Fig. 74 illustrates that specimens suddenly failed after substantial creep deformation. Similar to the cyclic loading, creep can reduce the strength if creep strain exceeds the strain corresponding to peak strength under monotonic loading. Fig. 75 demonstrates the time history of creep deformation. Evidently, the slow rate of creep distortion was transferred to abrupt deformation towards failure.

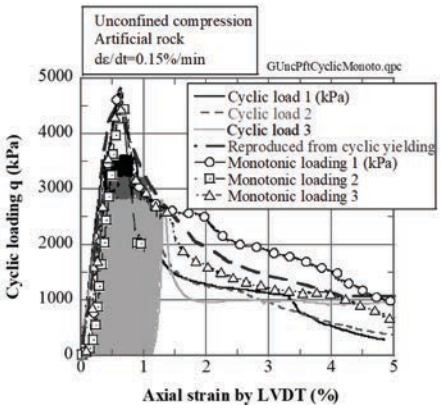

Figure 72. Effects of significant cyclic shear loading on deterioration of peak shear strength of artificial rock

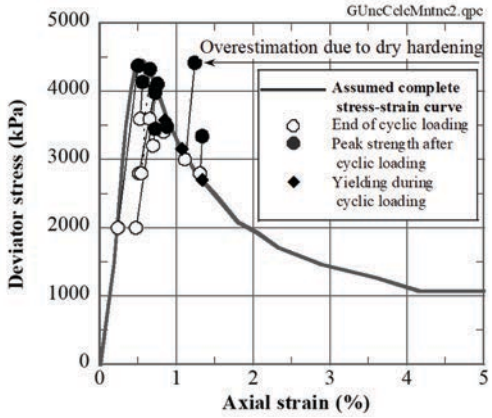

Figure 73. Relation of stress-strain states at the end of cyclic loading and at the peak strength during monotonic loading

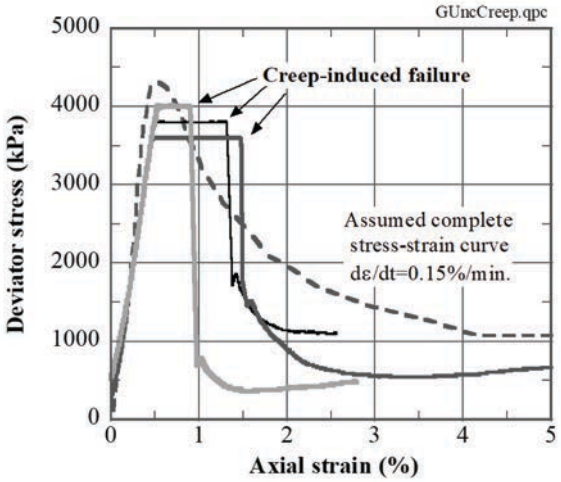

Figure 74. Deterioration of mechanical strength caused by creep deformation

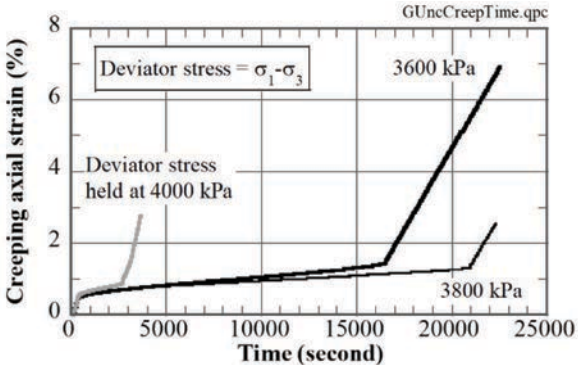

Figure 75. Deterioration of mechanical strength caused by creep deformation

8 SIZE OF PROCESS ZONE

The vulnerability of slopes to earthquake-induced landslides depends on many factors. Among them, the distance from the source of earthquake energy release (hypocenter, epicenter or fault rupture) plays a chief role. Hence, many efforts have been made to summarize case histories in order to show that there is an upper

bound distance beyond which landslide is unlikely (Yasuda, 1993). Moreover, Keefer (1984) showed that the greater earthquake magnitude increases the maximum distance to the slope failure. Obviously, this is because the greater magnitude means the greater seismic energy to be released.

Discussion on damage in rock caused by fault action directly develops to the concept of damage zone or process zone (Vermilye and Scholz, 1998). Fig. 76 illustrates the concept of process zone that is situated next to a slip plane and is of reduced mechanical strength as compared with the intact rock mass. To assess the size (width) of the process zone (distance measured from the fault), Vermilye and Scholz (1998) studied rock fissures around real fault while conducting literature reviews. Note that such a study is not easy because the size of the process (damage) zone may increase with the progress of accumulated fault dislocation (Savage and Brodsky, 2011).

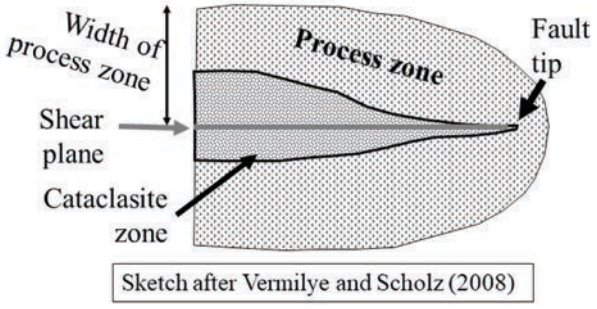

Figure 76. Schematic illustration of process zone proposed by Vermilye and Sholtz, 1998)

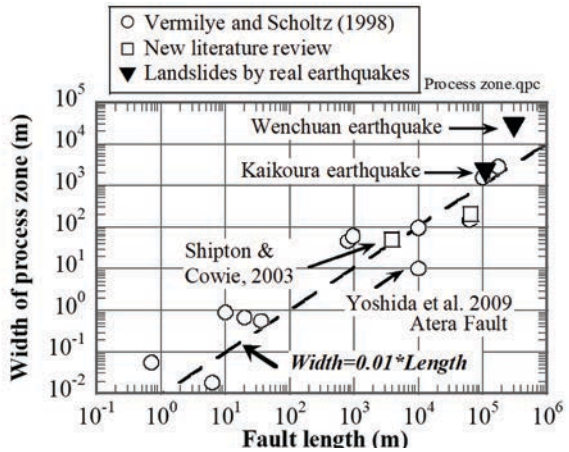

Figure 77. Assessed size of process zone (distance of damage measured from slip plane)

Qi et al. (2010) studied the effects of distance from the fault on the occurrence of landslides as well as the intensity of ground motion during the 2008 Wenchuan earthquake. It was found that the range of significant landslide occurrence was limited to -40 to +10 km of distance while intensity of ground motion had much bigger range. So, the present study assumes the mean size of landslide-prone area is (40+10)/2 = 25 km. The length of the causative fault is set equal to 300 km. As for the 2016 Kaikoura earthquake in New Zealand, Massey et al. (2018) studied more than 10,000 landslides and showed that the majority of slope failures are located within 2 km from the surface fault rupture. Because the Kaikoura earthquake was caused by a combined action of many faults, the present paper assumes 110 km that is the total length of the rupture zone.

All the data thus available are plotted in Fig. 76. It is interesting that the trend of the process zone size is consistent with the size of landslide zone along faults. Further study is required for this. Note that the distance from the fault is more useful than the epicentral distance when a fault is very long.

9 TSUNAMIGENIC SUBMARINE LANDSLIDES DURING EARTHQUAKES

Tsunami is mostly triggered by tectonic action in the ocean bed. However, another causative mechanism is submarine landslides. The 1964 Alaska earthquake of *M*w=9.2 caused a huge submarine landslide in the Inlet of Valdez and this abrupt change of submarine bathymetry induced huge tsunami (Fig. 78). The tsunami destroyed the town of Valdez and claimed 122 lives. Since the inlet is connected with the Pacific Ocean only through a narrow strait, it is reasonable that the tsunami originated inside the inlet (Coulter and Migliaccio, 1966).

The unstable submarine slope in the Valdez Inlet was made of rock flour (cohesionless silt) that was produced by glacier grinding in the mountain and was transported into the inlet by river. The fine grain size enabled very slow deposition of flour and loose cohesionless deposit was made in the sea. When the earthquake occurred, this material liquefied easily and the slope slipped.

The earthquake in Sulawesi Island in 2018 triggered submarine landslides in the Bay of Palu which in turn initiated tsunami. This tsunami affected the coastal region of Palu City (Fig. 79). Being different from the gigantic tsunami disasters in Sumatra (2004) and Tohoku (2011), the tsunami in Palu ran up only 100 meters or so on land probably because the volume of submarine

change of bathymetry was smaller. The 2016 Kaikoura earthquake in New Zealand caused tsunami as well whose height was 2 – 3 m in Kaikoura (Ministry of Civil Defence & Emergency Management, 2017). Furthermore, the tsunami disaster in 1998 in Papua New Guinea is attributed to seismically induced submarine landslides (Kawata et al., 1999; Tappin et al., 1999). Much is not yet known about the submarine landslides, whether seismic or non-seismic, and its hazard assessment is not in practice. Investigation on subaqueous landslide and tsunami deposit in Lake Luzern, Switzerland, revealed ancient earthquake in AD 1601 (Schnellmann et al., 2002).

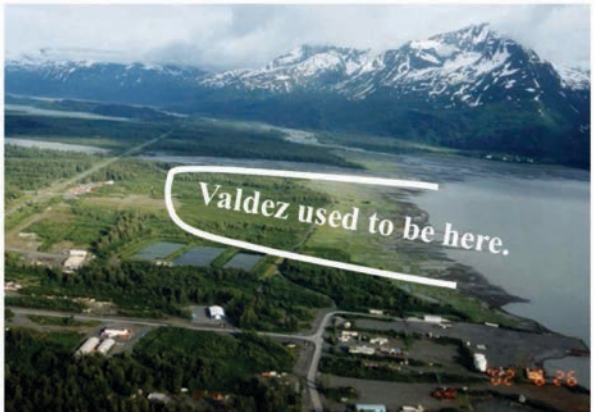

Figure 78. Valdez, Alaska, seen from airplane (photo by Dr. K. Horikoshi)

Figure 79. Palu, Sulawesi, Indonesia, after tsunami disaster

Figure 79. Aratozawa landslide caused by the 2008 Iwate-Miyagi Inland earthquake, Japan

The 2008 Iwate Miyagi Inland earthquake in Japan registered *M*w=6.8-6.9 and affected mountains in Tohoku Region. Because this region has many volcanos, the seismic instability of volcanic materials attracted attention. Fig. 80 illustrates one part of a gigantic Aratozawa landslide whose volume measured 67 million m^3 (Miyagi et al., 2011). According to Miyagi et al., this slide was of 700-m length, 800-m width and 70-80 meter thickness. It occurred along a flat slip plane of only 2-degree gradient that was made of volcanic materials.

Because the Aratozawa landslide occurred in the upstream catchment of Aratozawa Dam (Fig. 81), one part of the sliding mass moved into reservoir and triggered tsunami. Although this situation was similar to the tragedy of Vajont Dam in Italy, the tsunami was not very high and the dam was not damaged (Fig. 82). It was then understood that seismic instability of mountain slopes around reservoir needs more attention.

Figure 81. Aratozawa landslide as viewed beyond reservoir from the Aratozawa rockfill dam of 74.4-meter height

Figure 82. Aratozawa rockfill dam after the earthquake

10 NON-ENGIEERING WISDOM OF PEOPLE

Defending human community from the threat of earthquake-induced landslides is a common desire of people who are living in vulnerable areas. It is, however, still difficult to achieve this goal because of the following reasons;

- Earthquake cannot be foreseen and hence earthquake-induced landslide cannot be predicted, as stated before. This implies that warning-evacuation strategy does not work.
- Strong earthquake is a rare event. People do not like expenditures against it. This is in clear contrast to construction of infrastructures and buildings that accept expensive earthquake-resistant design.
- Subsurface investigation in mountain and sloping ground is tedious, costly and seldom practiced. Hence, information on shear strength of the ground is insufficient. This means that seismic stability analysis is not very reliable. Hazard mapping is carried out without good subsurface information.

Figure 83. Location of houses avoiding earthquake-induced landslides (2004 Niigata-Chuetsu earthquake, Japan)

Figure 84. Different locations of old and new houses (near Thimphu, Bhutan)

Accordingly, the choice is to avoid living in a vulnerable place. In other words, people should live away from unstable slopes. However, this is sometimes difficult for people living in narrow valleys in mountainous regions.

Away from the abovementioned negative remarks, it is interesting to pay attention to non-engineering human wisdom. After living in vulnerable regions for centuries, human has learned lessons from many unfortunate experiences. Fig. 83 shows the situation in Japan after landslide disasters caused by an earthquake. It deserves attention that people's houses (blue circles) were not affected by soil slips (red squares). After 1000-year history of the village I which man disasters occurred, people have learnt safe places to live. The same is found in Fig. 84 in which old houses are located behind woods and protected (to some extent) from debris flow in an alluvial fan. In contrast, new houses are situated in the center of a fan. Probably, modern people have forgotten the wisdom of ancestors and settled in open and comfortable places. Wisdom of our ancestors is not taught in engineering schools. We may have lost something very valuable.

11 CONCLUSION

This paper addresses the current state of knowledge and hard lessons learnt from landslides induced by earthquakes. Although many studies were done in the previous century, the gigantic earthquakes that started to occur since the end of the previous century demonstrated that there are still many issues unknown to human and that human have to do more efforts to mitigate the damage and risk. The conclusions drawn from this paper are described in what follows.

- The damage extent of earthquake-induced

landslides is significantly affected by water content, which in turn is influenced by the amount of antecedent rainfall.

- Safety measure in future should consider, thus, the compound effects of rainfall and earthquake.
- Landslide dam attracts more attention nowadays.
- Submarine landslides can trigger tsunami in the coastal region.
- There are construction geo-materials that are weak to water effect (slaking) and are not relevant for use.
- The long-term slope instability and related disasters are serious threats to local community after gigantic earthquakes.
- Some of the long-term instabilities are related with damage or process zone in rock near faults. It seems that past fault dislocation produced fissures and cracks in the rock body that result in huge landslide during strong earthquakes and long-term instability for years or decades after the earthquake.
- Minor shaking or creep deformation can cause damage in rock mass and, if occurring to a substantial extent, reduces the strength of rock.
- Because of the geometric amplification, the acceleration at the mountain top is stronger than at the foot. This can trigger failure mechanism of mountain body that is different from the conventional idea of shear failure. Tensile failure and toppling failure should be taken into account.
- Volcanic slopes are highly prone to seismic disturbance because it is not solid and can hold substantial amount of water. Even volcanic ash can hold water and gets fluidized upon seismic loading.
- The *H/L* data of earthquake-induced landslides suggests that frictional resistance of failed mass may be smaller than that of gravitationally induced landslide mass.
- One of the recent earthquakes triggered a long-distance flow in four slopes in a similar geological setting. Since such an extreme flow failure hardly happened during past earthquakes, its mechanism has to be understood urgently.
- Because the size of rupture zone of gigantic earthquakes is huge, the distance from the seismic source is accounted for more reasonably by distance to the rupture zone (fault) than the conventional epicentral distance. From this viewpoint, similarity was found between the idea of process zone and distribution of landslides around long causative faults.
- Development of modern technology did not take care of traditional non-engineering human wisdom for safety.

REFERENCES

Barrantes-Castillo, G., Jiménez-Campos, C., Ocón-García, M. J., (2013). "*Deslizamientos provocados por el terremoto de Cinchona de 2009, Costa Rica*". Revista Geográfica de América Centra,l 2(51): 89-100 (in Spanish).

Chang, K. J., Taboada, A., Chan, Y. C., (2005). "*Geological and morphological study of the Jiufengershan landslide triggered by the Chi-Chi Taiwan earthquake*". Geomorphology 71(3-4): 293-309.

Chigira, M., Nakasuji, A., et al. (2012). "*Soilslide-avalanches of pyroclastic fall deposits induced by the 2011 off the Pacific Coast of Tohoku earthquake*". Journal of the Japan Society of Engineering Geology, 52(6): 222-230 (in Japanese).

Costa, J. E., Schuster, R.L., (1988). "*The formation and failure of natural dams*". Geological Society of America Bulletin, 100(7): 1054-1068.

Coulter, H. W., Migliaccio, R. R., (1966). "*Effects of the earthquake of March 27, 1964 at Valdez, Alaska*". US Geological Survey Professional Report 542-C.

Dellow, S., Massey, C., McColl, S., Townsend, D., Villeneuve, M., (2017). "*Landslides caused by the 14 November 2016 Kaikoura earthquake, South Island, New Zealand*". Bulletin of the New Zealand Society of Earthquake Engineering, 50(2): 106-116.

Ermini, L., Casagli, N., (2002). "*Criteria for a preliminary assessment of landslide dam evolution*". Landslides - Proceedings of 1st European Conference on Landslides, 157-162.

Hayakawa, Y., Morita, T., Nakashimada, E., Kabe, N., (2002). *"The AD 818 Earthquake described in Ruiju Kokushi, and its geologic evidence printed on the southern foot of Akagi Volcano*". Historical Earthquakes, 18: 34-41 (in Japanese).

Hsu, P. S. T. (2012). "*Tsengwen reservoir siltation problem and remedial strategy.*". Material prepared by GT International, Taiwan.

Hsü, K. J. (1975). "*Catastrophic debris streams (Sturzstroms) generated by rockfalls*". Geological Society of America Bulletin 86: 129-140.

Hung, J. J., (2000). "*Chi-Chi earthquake induced landslides in Taiwan*". Earthquake Engineering and Engineering Seismology 2(2): 25-33.

Irsyam, M., Hanifa, N .R. et al. (2018). "*Damages associated with geotechnical problems in 2018 Palu*

earthquake, Indonesia". 20th Southeast Asian Geotechnical Conference, Jakarta, 5-14.

Jibson, R. W., Allstadt, K. E., Rengers, F. K., Godt, J. W., (2017). "*Overview of the geologic effects of the November 14, 2016, Mw 7.8 Kaikoura, New Zealand, earthquake*". USGS, Scientific Investigations Report 2017-5146.

Kanagawa Prefectural Government (1986). "*Prediction of seismic damage in Kanagawa Prefecture*". pp. 13-63 (in Japanese).

Kawata, S., (1943). "*Untersuchung des neuen Sees gebildet nach Erfolge des Erdbebens vom jahre 1941 im Formosa (Taiwan)*". Japanese Journal of Limnology, 13(1): 1-8 (in Japanese).

Kawata, Y., Benson, B. C., et al. (1999). "*Tsunami in Papua New Guinea was as intense as first thought*". EOS (Transactions, American Geophysical Union) 80: 101-105.

Kazama, M., Takamura, H., et al., (2006). "*Liquefaction mechanism of unsaturated volcanic sandy soils*". Proc. JSCE C 62(2): 546-561 (in Japanese).

Keefer, D. K. (1984). "*Landslides caused by earthquakes*". Geological Society of America Bulletin 95: 406-421.

Keefer, D. K., (1994). "*The importance of earthquake-induced landslides to long-term slope erosion and slope-failure hazards in seismically active regions*". Geomorphology 10(1-4): 265-284.

Kobayashi, Y. (1980). *"Slope hazards in recent earthquakes*". Journal of the Japan Society of Landslide, 17(1): 30-38 (in Japanese).

Kokusho, T. (2000). "*Mechanism of water film generation and lateral flow in liquefied sand layer*". Soils and Foundations 40(5): 99-111.

Konagai, K., Sattar, A., (2012). "*Partial breaching of Hattian Bala landslide dam formed in the 8th October 2005 Kashmir earthquake, Pakistan*". *Landslides*, *9*(1): 1-11.

Kurita, H., (2010). "*Introduction to the geology of the Chu-etsu area, Niigata Prefecture*". Chishitsu News 676: 28-31 (in Japanese).

Kurita, T., Annaka, T., (2005). "*Effect of irregular topography on strong ground motion amplification*". Proc. Japan Association for Earthquake Engineering, 5(3): 1-11.

Li, A. T., Huang, S. F., Song, X. N., (2012). "*Application of remote sensing monitoring in the typical landslide dammed lakes*". Yellow River Magazine, *34(*5): 78-81 (in Chinese).

Lin, C. W., Shieh, C. L., et al. (2004). "*Impact of Chi-Chi earthquake on the occurrence of landslides and debris flows: example from the Chenyulan River watershed, Nantou, Taiwan*". Engineering Geology 71: 49-61.

Lin, M. L., Wang, K. L., Chen, T. C., (2010). "*Debris flow hazard and mitigations in Taiwan following Chi-Chi earthquake, 1999*". Proc. 17th Southeast Asian Geotechnical Conference, Taipei, 123-136.

Lin, M. L., Chiang, T. K., (2019). "*Long term effects of landslides induced by catastrophic events*". 16th Asian Regional Conference on Soil Mechanics and Geotechnical Engineering, Taipei.

Massey, C., Della Pasqua, F., et al. (2017). "*Rock slope response to strong earthquake shaking*". Landslides, 14(1): 249-268.

Massey, C., Townsend, D., et al. (2018). "*Landslides Triggered by the 14 November 2016 Mw 7.8 Kaikoura Earthquake, New Zealand*". Bulletin of Seismological Society of America, 108(3B): 1630–1648.

Ministry of Civil Defence & Emergency Management, (2017). "*Kaikoura Earthquake and Tsunami: 14 November 2016*". Post Event Report (MEDEM Response).

Miyagi, T., Yamashina, S., et al. (2011). "*Massive landslide triggered by 2008 Iwate–Miyagi inland earthquake in the Aratozawa Dam area, Tohoku, Japan*". *Landslides*, *8*(1): 99-108.

Mokudai, K., Chigira, M., (2004). "*Geomorphic Features and Processes of Gravitational Mountain Deformation in the Area from Mt. Yambushi to Oya-Kuzure, Central Japan*". Geographical Review of Japan, The Association of Japanese Geographers, 77(2): 55-76 (in Japanese).

Mukunoki, T., Kasama, K., et al. (2016). "*Reconnaissance report on geotechnical damage caused by an earthquake with JMA seismic intensity 7 twice in 28 h, Kumamoto, Japan*". Soils and Foundations 56(6): 947-964.

Naumann, E. (1885). "*Über den Bau und die Entstehung der Japanischen Inseln*". publ. R. Friedländer & Sohn, Berlin (in German).

Qi, S. W., Xu, Q., Lan, H.X., Zhang, B., Liu, J.Y., (2010). "*Spatial distribution analysis of landslides triggered by 2008512 Wenchuan earthquake, China*". Engineering Geology 116(1-2): 95-108.

Savage, H. M., Brodsky, E. E., (2011). "*Collateral damage: Evolution with displacement of fracture distribution and secondary fault strands in fault damage zones*". Journal of Geophysical Research, 116(B3): B03405.

Schnellmann, M., Anselmetti, F. S., et al. (2002). "*Prehistoric earthquake history revealed by lacustrine slump deposits*". Geology by Geological Society of America, 30(12): 1131-1134.

Shipton, Z. K., Cowie, P. A., (2003). "*A conceptual model for the origin of fault damage zone structures in high-porosity sandstone*". Journal of Structural Geology, 25(3): 333-344.

Tabata, S., Mizuyzma, T., Inoue, K., (2002). "*Natural dam and disasters*". publ. Kokin Shoin, pp.50-53 (in Japanese).

Tang, C., Zhu, J., et al. (2011). "*Landslides induced by the Wenchuan earthquake and the subsequent strong rainfall event: A case study in the Beichuan area of China*". Engineering Geology, 122(1-2): 22-33.

Tappin, D. R., Matsumoto, T., et al. (1999). "*Sediment slump likely caused 1998 Papua New Guinea tsunami*". EOS (Transactions, American Geophysical Union) 80: 329-340.

Towhata, I., (2008). "*Derivation of formula for apparent frictional angle*". Section 15.9, Geotechnical Earthquake Engineering, Springer.

Towhata, I. (2019). "*Summarizing geotechnical activities after the 2011 Tohoku earthquake of Japan*". 7th Int. Conf. Earthquake Geotechnical Engineering, Ishihara Lecture, Rome.

Towhata, I., Gunji, K., (2018). "Long-term instability of slopes along major seismic faults". Keynote lecture at the 5th International Symposium on Mega Earthquake Induced Geo-disasters and Long Term Effects, Chengdu, May.

Tsuchiya, S., Imaizumi, F., (2010). "*Large sediment movement caused by the catastrophic Ohya-Kuzure landslide*". Journal of Disaster Research, 5(3): 257-263 (in Japanese).

Vermilye, J. M., Scholz, C. H., (1998). "*The process zone: a microstructural view of fault growth*". Journal of Geophysical Research, 103(B6): 12223-12237.

Wang, W. N., Wu, H. L., et al. (2003). "*Mass movements caused by recent tectonic activity: the 1999 Chi-Chi earthquake in central Taiwan*". The Island Arc, 12(4): 325-334.

Wang, L. M., Yuan, Z. X., et al. (2010). "*Criterions, prediction and prevention of loess liquefaction*". 5th Int. Conf. on Recent Advances in Geotechnical Earthquake Engineering and Soil Dynamics, San Diego, Paper No. OSP11.

Yagi, H., Yamasaki, T., Atsumi, M., (2007). "*GIS analysis on geomorphological features and soil mechanical implication of landslides caused by 2004 Niigata Chuetsu earthquake*". Journal of the Japan Landslide Society. 43: 294-306 (in Japanese).

Yasuda, S., (1993). "*Zoning for slope instability, Manual for zonation on seismic geotechnical hazards*". Technical Committee 4, Int. Soc. Soil Mech. Found. Engg., p. 49.

Yoshida, E., Oshima, A., et al., (2009). "*Fracture characterization along the fault - a case study of 'damaged zone' analysis on Atera Fault, Central Japan -*". Journal of Japan Society of Engineering Geology, 50(1): 16-28 (in Japanese).

Zhang, D., Wang, G., (2007). "*Study of the 1920 Haiyuan earthquake-induced landslides in loess (China)*". Engineering Geology, 94(1-2), pp.76-88.

Zhang, D., Wang, G., Luo, C., Chen, J., Zhou, Y., (2009). "*A rapid loess flowslide triggered by irrigation in China*". Landslides, 6(1), 55-60.